Published in final edited form as:
J Alzheimers Dis. 2009 April ; 16(4): 715–729. doi:10.3233/JAD-2009-0984.

Hepatic Ceramide May Mediate Brain Insulin Resistance and Neurodegeneration in Type 2 Diabetes and Non-alcoholic Steatohepatitis

Lascelles E. Lyn-Cook Jr[1], **Margot Lawton**[1], **Ming Tong**, **Elizabeth Silbermann**, **Lisa Longato**, **Ping Jiao**, **Princess Mark**, **Jack R. Wands**, **Haiyan Xu**, and **Suzanne M. de la Monte**[*]

Departments of Medicine, Pathology, and Clinical Neuroscience, Divisions of Gastroenterology and Endocrinology, and the Liver Research Center, Rhode Island Hospital and the Warren Alpert Medical School of Brown University, Providence, RI, USA

Abstract

Obesity, type 2 diabetes mellitus (T2DM), and non-alcoholic steatohepatitis (NASH) can be complicated by cognitive impairment and neurodegeneration. Experimentally, high fat diet (HFD)-induced obesity with T2DM causes mild neurodegeneration with brain insulin resistance. Since ceramides are neurotoxic, cause insulin resistance, and are increased in T2DM, we investigated the potential role of ceramides as mediators of neurodegeneration in the HFD obesity/T2DM model. We pair-fed C57BL/6 mice with a HFD or control diet for 4–20 weeks and examined pro-ceramide gene expression in liver and brain and neurodegeneration in the temporal lobe. HFD feeding gradually increased body weight, but after 16 weeks, liver weight surged ($P < 0.001$) due to lipid (triglyceride) accumulation ($P < 0.001$), and brain weight declined ($P < 0.0001$-Trend analysis). HFD feeding increased ceramide synthase, serine palmitoyl transferase, and sphingomyelinase expression in liver ($P < 0.05 – P < 0.001$), but not brain. In HFD fed mice, temporal lobe levels of ubiquitin ($P < 0.001$) and 4-hydroxynonenal ($P < 0.05$ or $P < 0.01$) increased, and tau, β-actin, and choline acetyltransferase levels decreased ($P < 0.05 – P < 0.001$) with development of NASH. In obesity, T2DM, or NASH, neurodegeneration with brain insulin resistance may be mediated by excess hepatic production of neurotoxic ceramides that readily cross the blood-brain barrier.

Keywords

Alzheimer's disease; amyloid; diabetes mellitus; high fat diet; insulin resistance; neurodegeneration; non-alcoholic steatohepatitis; obesity

INTRODUCTION

The prevalence rates of Alzheimer's disease (AD), obesity, type 2 diabetes mellitus (T2DM), and nonalcoholic fatty liver disease (NAFLD)/non alcoholic steatohepatitis (NASH), which includes metabolic syndrome, have all increased dramatically over the past several decades [1–6]. The probable inter-relatedness among these diseases is suggested by studies demonstrating: 1) increased risk of developing mild cognitive impairment (MCI), dementia,

[*] Corresponding author: Dr. Suzanne M. de la Monte, Rhode Island Hospital, 55 Claverick Street, 4th Floor, Providence, RI 02903, USA. Tel.: +1 401 444 7364; Fax: +1 401 444 2939; Suzanne_DeLaMonte_MD@Brown.edu.
[1]These authors contributed equally to this work.

or AD in individuals with T2DM [7,8]or obesity/dyslipidemic disorders [9]; 2) progressive brain insulin resistance and insulin deficiency in AD [10–13]; 3) cognitive impairment in experimental animal models of T2DM and/or obesity [14,15]; 4) AD-type neurodegeneration and cognitive impairment in experimentally induced brain insulin resistance and insulin deficiency [16–20]; 5) improved cognitive performance in experimental models of AD [21] and in human subjects with AD or MCI after treatment with insulin sensitizer agents or intranasal insulin [22–27]; and 6) similar molecular, biochemical, and mechanistic abnormalities in T2DM, NASH, and AD [7,28–33]. Since obesity,MCI, AD, T2DM, and NASH are all associated with insulin resistance, i.e., impaired ability to respond to insulin stimulation, they may share common etiologies. On the other hand, the lack of complete overlap among these disease states suggests that specific organ systems may be differentially afflicted by the same or similar exposures, resulting in dissimilar degrees of insulin resistance with disparate long-term outcomes, e.g., neurodegeneration versus NASH.

While aging is clearly the strongest risk factor for AD, emerging data suggest that T2DM and dyslidemic states can either contribute to, or serve as co-factors in its pathogenesis [34]. This concept is supported by epidemiologic data demonstrating a significant association between T2DM and MCI or dementia, and that T2DM is a significant risk factor for developingAD [7,35–39]. Mechanistically, increased risk of dementia in T2DM and obesity could be linked to chronic hyperglycemia, insulin resistance, oxidative stress, accumulation of advanced glycation end-products, increased production of pro-inflammatory cytokines, and/or microvascular disease [35]. However, most of these features define the core abnormalities in T2DM and NASH [40–43]. This concept led us to hypothesize that toxic/injurious agents produced in the body and associated with increased body mass index (BMI), mediate similar adverse effects in different target organs and tissues. Injurious agents or toxins causing insulin resistance in adipose tissue and skeletal muscle would result in T2DM, whereas the same insult in liver would produce NASH/metabolic syndrome, and in brain, MCI or early AD-type neurode-generation. We now propose that ceramides and related molecules are critical agents involved in the pathogenesis of these disease states because they: 1) can be generated in liver, adipose tissue, or brain [44–47]; 2) cause insulin resistance [45]; 3) are cytotoxic [45]; 4) increase in the central nervous system (CNS) with various dementia-associated diseases, including AD [46,48–50]; and 5) are lipid soluble and therefore likely to readily cross the blood-brain barrier.

By way of review, ceramides comprise a family of lipids generated from fatty acid and sphingosine (see reviews [45,51,52]). Ceramides are largely distributed in cell membranes, and in addition to their structural functions, ceramides have key roles in intracellular signaling and regulate growth, proliferation, cell migration, adhesion, growth arrest, differentiation, senescence, and apoptosis. Ceramides are generated by either *de novo* biosynthesis, or sphingolipid degradation (Table 1). For *de novo* synthesis, ceramides are produced from sphingosine or sphinganine plus fatty acyl-CoA through the actions of ceramide synthases [44,47,53]. Activation of serine palmitoyl transferase [44,45,54] or dihydroceramide synthase increases ceramide production in the endoplasmic reticulum via dihydroceramide desaturase (Table 1). Glycosphingolipids are composed of ceramide (hydrophobic) plus oligosaccharide (hydrophilic), and generated enzymatically in the Golgi [55–57]. UDP glucoceramide gycosyltransferase mediates the first step in transferring glucose from UDP-glucose to ceramide [55]. Ceramides also can be generated by hydrolysis of sphingomyelin by sphingomyelinase [44,52], or degradation of complex sphingolipids and glycosphingolipids localized in late endosomes and lysosomes [51]. Potential roles for ceramides in diabetes, obesity, inflammation, NASH, and neurodegeneration have already been suggested [45,46, 49,58]. Of note is that pro-inflammatory cytokines, such as tumor necrosis factor-alpha (TNF-α), can induce ceramide synthesis [45], and TNF-α levels are increased in both T2DM and NASH [59–62]. We investigated the potential role of ceramides as mediators of

neurodegenerationand brain insulin resistance utilizing an *in vivo* model of chronic obesity/T2DM [63].

MATERIALS AND METHODS

Obesity/T2DM model

Harlan adult male C57BL/6 mice (N = 10 per group), starting at 4 weeks of age, were pair-fed for 4, 8, 12, 16, or 20 weeks with high fat (HFD) chow diets in which 60% of the calories were derived from fat (Research Diets Inc, New Brunswick, NJ), or low fat (LFD) chow diets in which 5% of the calories were from fat (Harlan, Indianapolis, IN) as reported previously [63, 64]. Mice were weighed weekly, and at the time of sacrifice, fresh liver and brain weights were obtained. Livers and brains were sectioned for snap freezing and immersion fixation [63]. Fixed tissues were embedded in paraffin, and histological sections (8 microns) were stained with Hematoxylin and eosin (H&E; liver) or Luxol fast blue, H&E (brain). Frozen tissue was stored at −80°C for biochemical and molecular studies. Our experimental protocol was approved by the Institutional Animal Care and Use Committee at the Lifespan-Rhode Island Hospital and conforms to guidelines established by the National Institutes of Health.

Quantitative reverse transcriptase polymerase chain reaction (qRT-PCR) assay of gene expression

We used qRT-PCR to measure pro-ceramide gene expression with previously described methods [16]. Total RNA isolated from liver and temporal lobe was reverse transcribed using random oligodeoxynucleotide primers. The resulting cDNA templates were used in qPCR amplification reactions with gene specific primer pairs (Table 2) [16]. PCR amplifications were performed in 20 μl reactions containing cDNA generated from 2.5 ng of original RNA template, 300 nM each of gene specific forward and reverse primer, and 10 μl of 2x QuantiTect SYBR Green PCR Mix (Qiagen Inc, Valencia, CA). The amplified signals from triplicate reactions were detected and analyzed using the Master-cycler ep realplex instrument and software (Eppendorf AG, Hamburg, Germany). The amplification protocol used was as follows: initial 15-minutes denaturation and enzyme activation at 95°C, 40 cycles of 95°C × 15 sec, 55–60°C × 30 sec, and 72°C × 30 sec. Post-PCR melting points were examined for all samples. Annealing temperatures were optimized using the temperature gradient program provided with the software. The mRNA levels were determined using the equations of the regression lines generated with serial 10-fold dilutions of 20 ng of recombinant plasmid DNA containing the target sequences studied. Relative mRNA abundance was determined from the ng ratios of specific mRNA to18S [65,66]. PCR amplification efficiencies were all greater than 95%. Relative mRNA abundance was calculated from the ng ratios of specific mRNA to 18S rRNA measured in the same samples. Inter-group statistical comparisons were made using the calculated mRNA/18S ratios. 18S rRNA values were used as denominators because the large abundance of 18S provides an excellent loading control that is virtually invariant with disease state or experimental condition. Moreover, expression levels of traditional housekeeping genes, e.g., actin, glyceraldehyde 3 phosphate de-hydrogenase, and cyclophilin shift unpredictably with disease and experimental treatments, rendering them unreliable for normalizing data with respect to specific genes of interest.

Enzyme-Linked Immunosorbant Assay (ELISA)

Temporal lobes were homogenized in radioimmuno-precipitation assay buffer with protease and phosphatase inhibitors [16]. Protein concentrations were determined using the bicinchoninic acid (BCA) assay (Pierce, Rockford, IL). We used direct ELISAs to measure tau, phospho-tau, 4-hydroxy-2-nonenal (4-HNE), ubiquitin, β-actin, and choline acetyltransferase (ChAT) expression as previously described [67]. Immunoreactivity was detected with horseradish peroxidase (HRP)-conjugated secondary antibody and Amplex Red

soluble fluorophore [67]. Fluorescence was measured (Ex 579/Em 595) in a SpectraMax M5 microplate reader (Molecular Devices Corp., Sunnyvale, CA). Parallel negative control assays included incubations in which the primary, secondary, or both antibodies were omitted.

Lipid assays

Frozen tissues (50–70 mg each) were homogenized in 100 μl of water, and 10 μl aliquots were used to measure protein concentration with the BCA assay. Lipids were extracted by adding 1 ml chloroform-methanol (2:1) and incubating the samples for 1 h at room temperature with intermittent agitation. After centrifuging at 3000 rpm for 5 minutes at room temperature, the lipid-containing lower phase was transferred to a clean tube and air-dried. Pellets were re-suspended in 100 μl of 100% ethanol. Total lipid content was measured using a Nile Red fluorescence-based assay (Molecular Probes, Eugene, OR) [68–70]. Briefly, 5 μl aliquots of lipid extract were added to 190 μl of phosphate-buffered saline (PBS) in a 96-well polystyrene white plate, then 5 μl of Nile Red solution (1 mg/ml in DMSO) was added to each well. Reactions were light protected with aluminum foil and incubated at room temperature for 10 minutes with constant platform agitation. Fluorescence intensity (Ex 485/Em 572) was measured in a Spectra-Max M5 microplate reader. Triglyceride levels were measured using a Serum Triglyceride Determination kit (Sigma-Aldrich Co., St. Louis, MO), and cholesterol was measured using the Amplex Red Cholesterol Assay Kit (Molecular Probes, Eugene, OR) according to the manufacturers' protocols.

Source of reagents

QuantiTect SYBR Green PCR Mix was obtained from (Qiagen Inc, Valencia, CA). Rabbit or goat generated monoclonal or polyclonal antibodies to ubiquitin, tau, phospho-tau, 4-HNE, ChAT, and β-actin was purchased from Chemicon (Tecumsula, CA), Cal-Biochem (Carlsbad, CA) or Molecular Probes (Eugene, OR). Secondary antibodies were purchased from Pierce Chemical Co. (Rockford, IL). Amplex Red reagent was obtained from Molecular Probes (Eugene,OR). All other fine chemicals were purchased from either Cal-Biochem (Carlsbad, CA) or Sigma-Aldrich (St. Louis, MO).

Statistical analysis

Data depicted in the graphs represent the means ± S.E.M.'s for each group. Inter-group comparisons were made using Two-way Analysis of Variance (ANOVA) with the Bonferroni post-hoc test, or the post-hoc Deming test for linear trend. Statistical analyses were performed using GraphPad Prism 5 (GraphPad Software, Inc., San Diego, CA). The computer software generated significant P-values are indicated within the graph panels.

RESULTS

Longitudinal effects of the HFD on body, liver, and brain weights

The chronic HFD fed mice developed obesity and T2DM associated with fasting hyperglycemia, hyperlipidemia, and increased serum pro-inflammatory cytokine levels as previously reported [63,64]. Chronic HFD feeding caused progressive increases in mean body weight such that after 8 weeks, the HFD-fed mice were significantly heavier than the LFD control group. With increasing duration of HFD feeding, mean body weight continued to climb ($P < 0.0001$ for linear trend), whereas the mean body weight of the LFD group remained relatively stable (Fig. 1A), consistent with previous findings in this model [71]. During the first 12 weeks of study, HFD feeding had no significant effect on mean liver weight. Over that interval, the mean liver/body weight ratios were significantly lower in the HFD relative to LFD control group due to their progressive increases in body weight (data not shown). In contrast, at the 16 and 20 week time points, HFD-fed mice exhibited striking and significant increases

in mean liver weight (Fig. 1B) due to significant increases in hepatic lipid content as demonstrated with the Nile Red assay (Fig. 1C). Correspondingly, the calculated mean liver-body weight ratios were also increased relative to control (data not shown). Biochemical assays detected significantly elevated mean hepatic triglyceride content after 4, 16, and 20 weeks of HFD feeding (Fig. 1D), and significantly increased hepatic cholesterol after 20 weeks on the HFD (Fig. 1E).

Although mean brain weights were similar in the HFD and LFD groups after 4, 8, 12, 16, or 20 weeks of paired feeding (Fig. 1F), a time-dependent trend of declining mean brain weight was observed in the HFD ($R^2 = 0.475$; $P < 0.0001$), but not the LFD group (Fig. 1G–1H). The combined effects of increasing body mass and declining brain weight resulted in significantly reduced mean brain/body mass ratios in the HFD relative to control at the 8, 12, 16, and 20 week time points (Fig. 1I). The time dependent trend of declining brain weight/body weight ratio was also statistically significant ($P < 0.0001$). Finally, the sharpest reductions in brain/body weight ratio occurred concurrently with the striking increases in hepatic steatosis.

Chronic HFD feeding causes non-alcoholic steatohepatitis (NASH)

LFD livers exhibited regular cord-like architecture with minimal or no evidence of inflammation, steatosis, or apoptosis (Fig. 2). In contrast, after 4, 8, or 12 weeks on the HFD, the livers had progressive increases in hepatic micro- and macrosteatosis with associated disorganization of the architecture (Fig. 2A–2F). After 16 weeks of HFD feeding, the livers exhibited more prominent macro- and microsteatosis with small cluster of lymphomononuclear inflammatory cells (Fig. 2G–2H). After 20 weeks on the HFD, the livers had established histopathological features of NASH, consisting of widespread micro- and macro-steatosis in hepatocytes (40–50% versus 5–10% at earlier time points), patchy lymphomononuclearcell inflammation, apoptosis, and necrosis (Fig. 2I–2J), corresponding with previous descriptions of this and closely related models [72–74].

Neurodegeneration after chronic HFD feeding

Histopathological studies were focused on analysis of the temporal lobes because they are major targets of AD neurodegeneration. 4, 8, or 12 weeks of HFD feeding produced no detectable effects on brain histopathology. However, 16 weeks of HFD feeding caused subtle histopathological abnormalities consisting of scattered foci of neuronal loss,apoptosis, or nuclear pyknosis,increased irregularity of neuropil spacing among neurons (consistent with cell loss), and mildly increased white matter gliosis, as previously described [63]. Immunohistochemical staining studies failed to detect neurofibrillary tangles, dystrophic neurites, senile plaques, or AβPP-Aβ deposits in plaques or vessels in any of the brains, corresponding with our previous observations [63]. After 20 weeks of HFD feeding, ongoing apoptosis in both the hippocampal formation and temporal neocortex was more conspicuous, as evidenced by cell loss, and increased lipid peroxidation (4-HNE immunoreactivity), and gliosis (GFAP immunoreactivity) in these regions (Fig. 3). In addition, temporal white matter in HFD fed mice exhibited increased gliosis and lipid peroxidation, reflecting fiber degeneration (Fig. 3), as occurs early in the course of AD [75].

Effects of HFD on ceramide gene expression in liver and brain

Exploratory studies demonstrated that normal liver expresses Ceramide synthases (CER) 1, 2, 4, and 5, UDP glucose ceramide glucosyltransferase (UGCG), serine palmitoyltransferase (SPTLC) 1 and SPTLC2, and sphingomyelin phosphodiesterase (SMPD) 1 and SMPD3 (see Table 1 for definitions). qRT-PCR analysis revealed significantly higher mean levels of CER2, CER4, SPTLC1, SPTLC2, SMPD1, and SMPD3 mRNA transcripts in HFD compared with LFD livers, after 12 weeks on the diets (Fig. 4). However, the pro-ceramide synthesis mRNA transcripts, i.e., CER2, CER4, SPTLC1, and SPTLC2, were increased mainly at the 12- and

16-week time points, just preceding or coinciding with the early stages of conspicuous hepatic steatohepatitis. Their expression returned to control levels (4-week time point) after 20 weeks on the HFD. UGCG mRNA levels increased in both groups between the 4- and 8-week time points, and then gradually there-after in the control group, in which peak levels were detected at the 16- and 20-week time points. Mice fed with the HFD had earlier peaks in hepatic UGCG (at 12 or 16 weeks), and significantly lower levels than control at the 20-week time point (Fig. 4E). In HFD-fed mice, SMPD1 and SMPD3 mRNA transcripts increased progressively over time, such that their mean levels were significantly higher than control at both the 16 and 20 week time points (Fig. 4). In contrast to CER and SPTLC, SMPD1 and SMPD3 generate ceramide through hydrolysis of sphingolipids [44,51,52]. Corresponding with the qRT-PCR results, preliminary ELISA studies demonstrated higher levels of ceramide immunoreactivity in HFD relative to LFD fed mice at the 12- (21016 ± 1730 versus 16759 ± 208; $P = 0.025$) and 16-week (15636 ± 472 versus 14151 ± 160; $P = 0.037$) time points (Mean ± S.E.M. values in arbitrary units; Student T-tests with 4 samples per group). A more detailed analysis of HFD-induced alterations in ceramide levels and characteristics in liver and brain is currently underway and will be presented in a future report.

We also used qRT-PCR to measure expression of the same pro-ceramide genes in temporal lobe samples (Fig. 5). Generally higher levels of CER2, CER5, UGCG, SPTLC2, SMPD1 and SMPD3 were detected in brain at earlier compared to later time points in the study. We interpreted this result to possibly reflect developmental or aging effects on the expression levels of these genes. At the 8 and/or 12 week time points, CER2, UGCG, SPTLC2, SMPD1 and SMPD3 were all expressed at significantly lower levels in HFD compared with LFD brains. In addition, at the 16 and/or 20 week time points, the mean levels of UGCG mRNA were also significantly lower in the HFD compared with LFD group (Fig. 5). Therefore, unlike liver, temporal lobe ceramide gene expression was not increased by chronic HFD feeding.

Effect of obesity/T2DM on molecular and biochemical indices of AD

AD-type neurodegeneration is associated with increased levels of AβPP, oxidative stress, ubiquitin, and phospho-tau, and reduced levels of tau and ChAT mRNA [11]. ELISAs performed with temporal lobe tissue demonstrated similar mean levels of tau, phospho-tau, β-actin, ubiquitin, and 4-HNE in the HFD and LFD groups at the 8 and 12 week time points (Fig. 6). Only ChAT immunoreactivity was significantly reduced in the HFD group during these early time periods (Fig. 6D). At the 16- and/or 20-week time points, the mean levels of tau, β-actin, and ChAT were significantly reduced, whereas the mean levels of ubiquitin and 4-HNE were significantly increased in temporal lobes of HFD fed relative to control mice (Fig. 6).

DISCUSSION

Previously, we demonstrated that chronic HFD feeding, which results in obesity and T2DM, causes relatively modest AD-type molecular and biochemical abnormalities in brain, including insulin resistance [63]. For the present study, we re-generated the model to examine the time course of altered gene expression in brain, as well as uncover potential mechanisms by which peripheral insulin resistance causes AD-type neurodegeneration. This line of investigation is important because it could lead to the discovery of biomarkers for detecting individuals at risk for developing cognitive impairment or progressing from MCI to AD in the context of obesity/T2DM. We focused our attention on the liver because previous studies showed that: 1) NASH occurs frequently with obesity/T2DM and is a feature of the model used herein; 2) NASH is associated with hepatic insulin resistance; 3) individuals with NASH can exhibit neuropsychiatric dysfunction, including anxiety and depression [76], which frequently precede cognitive impairment and dementia; 4) peripheral ceramide production is increased in adipose

tissue in NASH, and ceramides, as well as long-chain fatty acids, mediate insulin resistance [45,77,78]; and 5) ceramide can be neurotoxic, and its levels are increased in AD as well as other injury or inflammatory disease states [46,48–50,79,80].

This study demonstrated that HFD feeding caused body weight to increase progressively, and eventually achieve levels that were nearly two-fold higher than control. The indices of T2DM, including hyperglycemia, hyperinsulinemia, and hypercholesterolemia also increased progressively over the time course of HFD feeding as previously reported [64,81]. In contrast, liver weight remained relatively stable during the first 12 weeks of feeding, but then increased sharply after 16 and 20 weeks of HFD feeding, due to striking increases in hepatic lipid content (steatosis), inflammation, apoptosis, and necrosis, i.e., NASH. Other investigators demonstrated that NASH, in this or related models, is associated with increased serum transaminase levels, reflecting hepatocellular injury [72,74,82]. Therefore, it appears that during the earlier phases of HFD feeding, compensatory mechanisms help sustain structural and functional integrity of the liver, but after 16 weeks of HFD feeding, a critical metabolic perturbation disrupts the homeostatic milieu, allowing hepatic steatosis to progress to NASH. One potential mediator of this response is the abrupt surge in serum TNF-α that occurs after 16 weeks of HFD feeding [83]. TNF-α is a potent pro-inflammatory cytokine that plays a key role in peripheral and hepatic insulin resistance [60,62,84,85], and also promotes ceramide biosynthesis [45]. Although a potential source of the increased TNF-α in this model is peripheral adipose tissue with ongoing adipocyte death and remodeling [83], preliminary data suggest that endogenous hepatic TNF-α expression is increased in the HFD mice (Longato, et al, unpublished).

After 16 weeks of HFD feeding, the livers exhibited histopathological features of NASH, i.e., steatosis with multiple foci of lymphomononuclear cell inflammation, necrosis, and apoptosis, consistent with previous reports [74]. Molecular studies demonstrated that throughout the period of HFD feeding, the mRNA levels of various pro-ceramide genes were significantly increased relative to control, including genes responsible for generating ceramide *de novo* (CER 2,3,4,5), and also those involved in sphingomyelin degradation (SMPD1 and SMPD3). The gradual reductions in the expression of genes that mediate *de novo* ceramide synthesis could represent a compensatory response to lipid accumulation in hepatocytes. On the other hand, the persistently increased levels of SMPD3 after 16 or 20 weeks of HFD feeding may reflect an effort to prevent further accumulation of lipids in hepatocytes through increased hydrolysis of sphingomyelin.

Consequences of increased sphingomyelinase activity include increased generation of ceramide through degradation of sphingmyelin, as well as increased production of fatty acids. Since ceramides have key roles in signaling cellular processes such as growth arrest, senescence, apoptosis, and cell death, increased expression of pro-ceramide genes could contribute to the deficits in hepatocellular repair and regenerative functions in NASH [45, 77]. Conceivably, ceramides generated by degradation of sphingolipids and glycosphingolipids localized in late endosomes and lysosomes may be more toxic and inhibitory to insulin signaling than ceramides generated via *de novo* synthesis pathways [45,58,77]. In contrast to the findings in liver, temporal lobe (brain) pro-ceramide gene expression was not significantly increased by the chronic HFD feeding. Therefore, if ceramides have a role in mediating brain insulin resistance, neurodegeneration, and cognitive impairment in obesity, T2DM, and NASH, the source is not likely to be the CNS, and instead would probably be of liver, and possibly adipocyte origin.

Previously, we demonstrated that chronic HFD feeding of C57BL/6 mice causes mild neuropathological lesions but significant impairments in insulin receptor binding and insulin responsive gene expression in temporal lobe tissue [63]. Those abnormalities were associated

with reduced expression of ChAT and GAPDH. The time course analysis performed in the present study revealed early impairments in ChAT expression, beginning after only 8 weeks of HFD feeding, and coinciding with the increases in the expression of multiple proceramide genes in liver. The facts that: 1) ceramide inhibits insulin signaling [45,77]; 2) ChAT gene expression is insulin responsive [86]; and 3) ceramide is lipid soluble and therefore probably readily crosses the blood brain barrier, suggest that the early impairments in ChAT expression in brain may be mediated by increased hepatic ceramide production. However, it is noteworthy that ChAT expression increased sharply between 4 and 8 weeks on the LFD, whereas in mice fed with the HFD, ChAT expression increased gradually over time, such that at the 16- and 20-week time points, the levels more closely approximated to those in the control group. This suggests that maturation of CNS cholinergic function may be delayed but not thoroughly impaired by brain insulin resistance states.

The other indices of neurodegeneration, including increased 4-HNE (marker of lipid peroxidation) and ubiquitin (index of abnormal protein processing and accumulation), and reduced tau (probably reflecting cytoskeletal collapse and insulin/IGF resistance) were primarily detected at the 16 and 20 week time points, coinciding with surges in steatohepatitis and serum TNF-α, and persistent elevation of hepatic SMPD3. These results provide supportive evidence that hepatic/peripheral ceramide and pro-inflammatory cytokine production play key roles in the pathogenesis of CNS oxidative stress, insulin resistance and neuronal cytoskeletal collapse, all of which occur in AD.

Since AD shares many biochemical, molecular, and signal transduction abnormalities in common with T2DM and NASH, but the relevant pathology is fundamentally confined to the CNS in the vast majority of cases, we suggested that AD be regarded as “Type 3 diabetes” [10,11]. It is of particular interest that, with regard to the antecedent discussion, CNS ceramide levels are elevated in both AD [49] and AD-relevant experimental animal models [46,79]. These relatively recent observations hearken back to a much earlier report showing that white matter atrophy is one of the earliest abnormalities in AD [75]. At the present time, it appears that white matter atrophy in AD could be mediated by brain insulin resistance, which is evident even in the early stages of AD [11]. Insulin resistance in white matter would result in degeneration and loss of oligodendroglia, since oligodendroglia require insulin/IGF-1 for survival signaling and myelinogenesis [87–89]. On the other hand, insulin/IGF resistance would promote oxidative stress and secondarily lead to activation of pro-inflammatory cascades in astrocytes, and attendant myelin degeneration via activation of sphingomyelinases and pro-inflammatory cytokines, including TNF-α, and attendant release of ceramide. This proposed scheme provides a mechanism for producing Type 3 diabetes without the need for hepatic/peripheral sources of ceramides or cytokines, and which would be relevant in the vast majority of sporadic AD cases. With mounting evidence pointing toward CNS insulin/IGF resistance as the mediator if not initiator of AD-type neurodegeneration, our very next goal should be to identify the agents and factors responsible for establishing this cascade.

Although a likely connection between increased CNS ceramide (and probably other toxic lipids as well) and AD has been demonstrated as discussed above, the novelty of the present work is that extra-CNS sources of ceramide, such as liver or adipose tissue, can contribute to the pathogenesis of cognitive impairment and AD-type neurodegeneration. The critical variable mediating this effect may be the degree to which liver disease or adipocyte degeneration and remodeling increase ceramide production. The fact that the effects of HFD feeding were not identical to that which actually happens in AD, lends support to our hypothesis that T2DM, NASH, and obesity do not cause AD, and instead they probably serve as pathogenic co-factors. This phenomenon could account for both the absence of complete overlap and the two- or three-fold increased risk of developing MCI or AD among individuals with T2DM [7–9]. Improved ability to detect increased levels of toxic ceramides and related lipids in peripheral

blood and cerebrospinal fluid may help identify individuals at risk for developing cognitive impairment in the context of obesity, T2DM, and/or NASH.

Acknowledgments

Research supported by AA02666, AA02169, AA11431, AA12908, and AA16126 from the National Institutes of Health, and a Child Health Research Grant from the Hood Foundation

REFERENCES

1. Rector RS, Thyfault JP, Wei Y, Ibdah JA. Non-alcoholic fatty liver disease and the metabolic syndrome: an update. World J Gastroenterol 2008;14:185–192. [PubMed: 18186553]
2. Pradhan A. Obesity, metabolic syndrome, and type 2 diabetes: inflammatory basis of glucose metabolic disorders. Nutr Rev 2007;65:S152–S156. [PubMed: 18240540]
3. Launer LJ. Next steps in Alzheimer's disease research: interaction between epidemiology and basic science. Curr Alzheimer Res 2007;4:141–143. [PubMed: 17430237]
4. Wang XP, Ding HL. Alzheimer's disease: epidemiology, genetics, and beyond. Neurosci Bull 2008;24:105–109. [PubMed: 18369390]
5. Delgado JS. Evolving trends in nonalcoholic fatty liver disease. Eur J Intern Med 2008;19:75–82. [PubMed: 18249301]
6. Nugent C, Younossi ZM. Evaluation and management of obesity-related nonalcoholic fatty liver disease. Nat Clin Pract Gastroenterol Hepatol 2007;4:432–441. [PubMed: 17667992]
7. Pasquier F, Boulogne A, Leys D, Fontaine P. Diabetes mellitus and dementia. Diabetes Metab 2006;32:403–414. [PubMed: 17110895]
8. Verdelho A, Madureira S, Ferro JM, Basile AM, Chabriat H, Erkinjuntti T, Fazekas F, Hennerici M, O'Brien J, Pantoni L, Salvadori E, Scheltens P, Visser MC, Wahlund LO, Waldemar G, Wallin A, Inzitari D. Differential impact of cerebral white matter changes, diabetes, hypertension and stroke on cognitive performance among non-disabled elderly. The LADIS study. J Neurol Neurosurg Psychiatry 2007;78:1325–1330. [PubMed: 17470472]
9. Martins IJ, Hone E, Foster JK, Sunram-Lea SI, Gnjec A, Fuller SJ, Nolan D, Gandy SE, Martins RN. Apolipoprotein E, cholesterol metabolism, diabetes, and the convergence of risk factors for Alzheimer's disease and cardiovascular disease. Mol Psychiatry 2006;11:721–736. [PubMed: 16786033]
10. Rivera EJ, Goldin A, Fulmer N, Tavares R, Wands JR, de la Monte SM. Insulin and insulin-like growth factor expression and function deteriorate with progression of Alzheimer's disease: link to brain reductions in acetylcholine. J Alzheimers Dis 2005;8:247–268. [PubMed: 16340083]
11. Steen E, Terry BM, Rivera EJ, Cannon JL, Neely TR, Tavares R, Xu XJ, Wands JR, de la Monte SM. Impaired insulin and insulin-like growth factor expression and signaling mechanisms in Alzheimer's disease–is this type 3 diabetes? J Alzheimers Dis 2005;7:63–80. [PubMed: 15750215]
12. Craft S. Insulin resistance and Alzheimer's disease pathogenesis: potential mechanisms and implications for treatment. Curr Alzheimer Res 2007;4:147–152. [PubMed: 17430239]
13. Craft S. Insulin resistance syndrome and Alzheimer disease: pathophysiologic mechanisms and therapeutic implications. Alzheimer Dis Assoc Disord 2006;20:298–301. [PubMed: 17132977]
14. Winocur G, Greenwood CE, Piroli GG, Grillo CA, Reznikov LR, Reagan LP, McEwen BS. Memory impairment in obese Zucker rats: an investigation of cognitive function in an animal model of insulin resistance and obesity. Behav Neurosci 2005;119:1389–1395. [PubMed: 16300445]
15. Winocur G, Greenwood CE. Studies of the effects of high fat diets on cognitive function in a rat model. Neurobiol Aging 2005;1(6 Suppl):46–49. [PubMed: 16219391]
16. Lester-Coll N, Rivera EJ, Soscia SJ, Doiron K, Wands JR, de la Monte SM. Intracerebral streptozotocin model of type 3 diabetes: relevance to sporadic Alzheimer's disease. J Alzheimers Dis 2006;9:13–33. [PubMed: 16627931]
17. Weinstock M, Shoham S. Rat models of dementia based on reductions in regional glucose metabolism, cerebral blood flow and cytochrome oxidase activity. J Neural Transm 2004;111:347–366. [PubMed: 14991459]

18. Nitta A, Murai R, Suzuki N, Ito H, Nomoto H, Katoh G, Furukawa Y, Furukawa S. Diabetic neuropathies in brain are induced by deficiency of BDNF. Neurotoxicol Teratol 2002;24:695–701. [PubMed: 12200200]
19. Hoyer S, Lannert H, Noldner M, Chatterjee SS. Damaged neuronal energy metabolism and behavior are improved by Ginkgo biloba extract (EGb 761). J Neural Transm 1999;106:1171–1188. [PubMed: 10651112]
20. Biju MP, Paulose CS. Brain glutamate dehydrogenase changes in streptozotocin diabetic rats as a function of age. Biochem Mol Biol Int 1998;44:1–7. [PubMed: 9503142]
21. de la Monte SM, Tong M, Lester-Coll N, Plater M Jr, Wands JR. Therapeutic rescue of neurodegeneration in experimental type 3 diabetes: relevance to Alzheimer's disease. J Alzheimers Dis 2006;10:89–109. [PubMed: 16988486]
22. Haan MN. Therapy Insight: type 2 diabetes mellitus and the risk of late-onset Alzheimer's disease. Nat Clin Pract Neurol 2006;2:159–166. [PubMed: 16932542]
23. Reger MA, Watson GS, Green PS, Wilkinson CW, Baker LD, Cholerton B, Fishel MA, Plymate SR, Breitner JC, Degroodt W, Mehta P, Craft S. Intranasal insulin improves cognition and modulates {beta}-amyloid in early AD. Neurology 2008;70:440–448. [PubMed: 17942819]
24. Landreth G. Therapeutic use of agonists of the nuclear receptor PPARgamma in Alzheimer's disease. Curr Alzheimer Res 2007;4:159–164. [PubMed: 17430241]
25. Watson GS, Bernhardt T, Reger MA, Cholerton BA, Baker LD, Peskind ER, Asthana S, Plymate SR, Frolich L, Craft S. Insulin effects on CSF norepinephrine and cognition in Alzheimer's disease. Neurobiol Aging 2006;27:38–41. [PubMed: 16298239]
26. Reger MA, Watson GS, Frey WH 2nd, Baker LD, Cholerton B, Keeling ML, Belongia DA, Fishel MA, Plymate SR, Schellenberg GD, Cherrier MM, Craft S. Effects of intranasal insulin on cognition in memory-impaired older adults: modulation by APOE genotype. Neurobiol Aging 2006;27:451–458. [PubMed: 15964100]
27. Pedersen WA, McMillan PJ, Kulstad JJ, Leverenz JB, Craft S, Haynatzki GR. Rosiglitazone attenuates learning and memory deficits in Tg2576 Alzheimer mice. Exp Neurol 2006;199:265–273. [PubMed: 16515786]
28. Nicolls MR. The clinical and biological relationship between Type II diabetes mellitus and Alzheimer's disease. Curr Alzheimer Res 2004;1:47–54. [PubMed: 15975085]
29. Yeh MM, Brunt EM. Pathology of nonalcoholic fatty liver disease. Am J Clin Pathol 2007;128:837–847. [PubMed: 17951208]
30. Marchesini G, Marzocchi R. Metabolic syndrome and NASH. Clin Liver Dis 2007;11:105–117. ix. [PubMed: 17544974]
31. Papandreou D, Rousso I, Mavromichalis I. Update on non-alcoholic fatty liver disease in children. Clin Nutr 2007;26:409–415. [PubMed: 17449148]
32. Pessayre D. Role of mitochondria in non-alcoholic fatty liver disease. J Gastroenterol Hepatol 2007;1 (22 Suppl):S20–S27. [PubMed: 17567459]
33. Wei Y, Rector RS, Thyfault JP, Ibdah JA. Nonalcoholic fatty liver disease and mitochondrial dysfunction. World J Gastroenterol 2008;14:193–199. [PubMed: 18186554]
34. Qiu C, De Ronchi D, Fratiglioni L. The epidemiology of the dementias: an update. Curr Opin Psychiatry 2007;20:380–385. [PubMed: 17551353]
35. Whitmer RA. Type 2 diabetes and risk of cognitive impairment and dementia. Curr Neurol Neurosci Rep 2007;7:373–380. [PubMed: 17764626]
36. Haan MN, Wallace R. Can dementia be prevented? Brain aging in a population-based context. Annu Rev Public Health 2004;25:1–24. [PubMed: 15015910]
37. Luchsinger JA, Mayeux R. Cardiovascular risk factors and Alzheimer's disease. Curr Atheroscler Rep 2004;6:261–266. [PubMed: 15191699]
38. Luchsinger JA, Reitz C, Patel B, Tang MX, Manly JJ, Mayeux R. Relation of diabetes to mild cognitive impairment. Arch Neurol 2007;64:570–575. [PubMed: 17420320]
39. Launer LJ. Diabetes and brain aging: epidemiologic evidence. Curr Diab Rep 2005;5:59–63. [PubMed: 15663919]

40. Garcia-Galiano D, Sanchez-Garrido MA, Espejo I, Montero JL, Costan G, Marchal T, Membrives A, Gallardo-Valverde JM, Munoz-Castaneda JR, Arevalo E, De la Mata M, Muntane J. IL-6 and IGF-1 are independent prognostic factors of liver steatosis and non-alcoholic steatohepatitis in morbidly obese patients. Obes Surg 2007;17:493–503. [PubMed: 17608262]

41. Gholam PM, Flancbaum L, Machan JT, Charney DA, Kotler DP. Nonalcoholic fatty liver disease in severely obese subjects. Am J Gastroenterol 2007;102:399–408. [PubMed: 17311652]

42. Liew PL, Lee WJ, Lee YC, Wang HH, Wang W, Lin YC. Hepatic histopathology of morbid obesity: concurrence of other forms of chronic liver disease. Obes Surg 2006;16:1584–1593. [PubMed: 17217634]

43. Nobili V, Manco M. Measurement of advanced glycation end products may change NASH management. J Gastroenterol Hepatol 2007;22:1354–1355. [PubMed: 17716339]

44. Shah C, Yang G, Lee I, Bielawski J, Hannun YA, Samad F. Protection from high fat diet-induced increase in ceramide in mice lacking plasminogen activator inhibitor 1. J Biol Chem 2008;283:13538–13548. [PubMed: 18359942]

45. Summers SA. Ceramides in insulin resistance and lipotoxicity. Prog Lipid Res 2006;45:42–72. [PubMed: 16445986]

46. Alessenko AV, Bugrova AE, Dudnik LB. Connection of lipid peroxide oxidation with the sphingomyelin pathway in the development of Alzheimer's disease. Biochem Soc Trans 2004;32:144–146. [PubMed: 14748735]

47. Laviad EL, Albee L, Pankova-Kholmyansky I, Epstein S, Park H, Merrill AH Jr, Futerman AH. Characterization of ceramide synthase 2: tissue distribution, substrate specificity, and inhibition by sphingosine 1-phosphate. J Biol Chem 2008;283:5677–5684. [PubMed: 18165233]

48. Nakane M, Kubota M, Nakagomi T, Tamura A, Hisaki H, Shimasaki H, Ueta N. Lethal forebrain ischemia stimulates sphingomyelin hydrolysis and ceramide generation in the gerbil hippocampus. Neurosci Lett 2000;296:89–92. [PubMed: 11108988]

49. Katsel P, Li C, Haroutunian V. Gene expression alterations in the sphingolipid metabolism pathways during progression of dementia and Alzheimer's disease: a shift toward ceramide accumulation at the earliest recognizable stages of Alzheimer's disease? Neurochem Res 2007;32:845–856. [PubMed: 17342407]

50. Adibhatla RM, Hatcher JF. Altered Lipid Metabolism in Brain Injury and Disorders. Subcell Biochem 2008;48 ihpa41041.

51. Liu B, Obeid LM, Hannun YA. Sphingomyelinases in cell regulation. Semin Cell Dev Biol 1997;8:311–322. [PubMed: 10024495]

52. Reynolds CP, Maurer BJ, Kolesnick RN. Ceramide synthesis and metabolism as a target for cancer therapy. Cancer Lett 2004;206:169–180. [PubMed: 15013522]

53. Mizutani Y, Kihara A, Igarashi Y. Mammalian Lass6 and its related family members regulate synthesis of specific ceramides. Biochem J 2005;390:263–271. [PubMed: 15823095]

54. Mari M, Fernandez-Checa JC. Sphingolipid signalling and liver diseases. Liver Int 2007;27:440–450. [PubMed: 17403183]

55. Paul P, Kamisaka Y, Marks DL, Pagano RE. Purification and characterization of UDP-glucose:ceramide glucosyltransferase from rat liver Golgi membranes. J Biol Chem 1996;271:2287–2293. [PubMed: 8567691]

56. Greco D, Kotronen A, Westerbacka J, Puig O, Arkkila P, Kiviluoto T, Laitinen S, Kolak M, Fisher RM, Hamsten A, Auvinen P, Yki-Jarvinen H. Gene expression in human NAFLD. Am J Physiol Gastrointest Liver Physiol 2008;294:G1281–G1287. [PubMed: 18388185]

57. Jennemann R, Sandhoff R, Wang S, Kiss E, Gretz N, Zuliani C, Martin-Villalba A, Jager R, Schorle H, Kenzelmann M, Bonrouhi M, Wiegandt H, Grone HJ. Cell-specific deletion of glucosylceramide synthase in brain leads to severe neural defects after birth. Proc Natl Acad Sci U S A 2005;102:12459–12464. [PubMed: 16109770]

58. Han MS, Park SY, Shinzawa K, Kim S, Chung KW, Lee JH, Kwon CH, Lee KW, Park CK, Chung WJ, Hwang JS, Yan JJ, Song DK, Tsujimoto Y, Lee MS. Lysophosphatidyl-choline as a death effector in the lipoapoptosis of hepatocytes. J Lipid Res 2008;49:84–97. [PubMed: 17951222]

59. Sahai A, Malladi P, Pan X, Paul R, Melin-Aldana H, Green RM, Whitington PF. Obese and diabetic db/db mice develop marked liver fibrosis in a model of nonalcoholic steatohepatitis: role of short-

form leptin receptors and osteopontin. Am J Physiol Gastrointest Liver Physiol 2004;287:G1035–G1043. [PubMed: 15256362]

60. Lieber CS, Leo MA, Mak KM, Xu Y, Cao Q, Ren C, Ponomarenko A, DeCarli LM. Model of nonalcoholic steatohepatitis. Am J Clin Nutr 2004;79:502–509. [PubMed: 14985228]
61. Yalniz M, Bahcecioglu IH, Ataseven H, Ustundag B, Ilhan F, Poyrazoglu OK, Erensoy A. Serum adipokine and ghrelin levels in nonalcoholic steatohepatitis. Mediators Inflamm 2006;2006:34295. [PubMed: 17392582]
62. Satapathy SK, Garg S, Chauhan R, Sakhuja P, Malhotra V, Sharma BC, Sarin SK. Beneficial effects of tumor necrosis factor-alpha inhibition by pentoxifylline on clinical, biochemical, and metabolic parameters of patients with nonalcoholic steatohepatitis. Am J Gastroenterol 2004;99:1946–1952. [PubMed: 15447754]
63. Moroz N, Tong M, Longato L, Xu H, de la Monte SM. Limited Alzheimer-type neurodegeneration in experimental obesity and Type 2 diabetes mellitus. J Alzheimers Dis 2008;15:29–44. [PubMed: 18780965]
64. Xu H, Barnes GT, Yang Q, Tan G, Yang D, Chou CJ, Sole J, Nichols A, Ross JS, Tartaglia LA, Chen H. Chronic inflammation in fat plays a crucial role in the development of obesity-related insulin resistance. J Clin Invest 2003;112:1821–1830. [PubMed: 14679177]
65. Yeon JE, Califano S, Xu J, Wands JR, De La Monte SM. Potential role of PTEN phosphatase in ethanol-impaired survival signaling in the liver. Hepatology 2003;38:703–714. [PubMed: 12939597]
66. Xu J, Eun Yeon J, Chang H, Tison G, Jun Chen G, Wands JR, De La Monte SM. Ethanol impairs insulin-stimulated neuronal survival in the developing brain: Role of PTEN phosphatase. J Biol Chem 2003;278:26929–26937. [PubMed: 12700235]
67. Cohen AC, Tong M, Wands JR, de la Monte SM. Insulin and insulin-like growth factor resistance with neurodegeneration in an adult chronic ethanol exposure model. Alcohol Clin Exp Res 2007;31:1558–1573. [PubMed: 17645580]
68. McMillian MK, Grant ER, Zhong Z, Parker JB, Li L, Zivin RA, Burczynski ME, Johnson MD. Nile Red binding to HepG2 cells: an improved assay for in vitro studies of hepatosteatosis. In Vitr Mol Toxicol 2001;14:177–190. [PubMed: 11846991]
69. Fowler SD, Greenspan P. Application of Nile red, a fluorescent hydrophobic probe, for the detection of neutral lipid deposits in tissue sections: comparison with oil red O. J Histochem Cytochem 1985;33:833–836. [PubMed: 4020099]
70. Greenspan P, Fowler SD. Spectrofluorometric studies of the lipid probe, nile red. J Lipid Res 1985;26:781–789. [PubMed: 4031658]
71. Winzell MS, Magnusson C, Ahren B. Temporal and dietary fat content-dependent islet adaptation to high-fat feeding-induced glucose intolerance in mice. Metabolism 2007;56:122–128. [PubMed: 17161234]
72. Cong WN, Tao RY, Tian JY, Liu GT, Ye F. The establishment of a novel non-alcoholic steatohepatitis model accompanied with obesity and insulin resistance in mice. Life Sci 2008;82:983–990. [PubMed: 18417155]
73. Yoshimatsu M, Terasaki Y, Sakashita N, Kiyota E, Sato H, van der Laan LJ, Takeya M. Induction of macrophage scavenger receptor MARCO in nonalcoholic steatohepatitis indicates possible involvement of endotoxin in its pathogenic process. Int J Exp Pathol 2004;85:335–343. [PubMed: 15566430]
74. Kirsch R, Clarkson V, Verdonk RC, Marais AD, Shephard EG, Ryffel B, de la MHP. Rodent nutritional model of steatohepatitis: effects of endotoxin (lipopolysaccharide) and tumor necrosis factor alpha deficiency. J Gastroenterol Hepatol 2006;21:174–182. [PubMed: 16706830]
75. de la, Monte SM. Quantitation of cerebral atrophy in preclinical and end-stage Alzheimer's disease. Ann Neurol 1989;25:450–459. [PubMed: 2774485]
76. Elwing JE, Lustman PJ, Wang HL, Clouse RE. Depression, anxiety, and nonalcoholic steatohepatitis. Psychosom Med 2006;68:563–569. [PubMed: 16868265]
77. Holland WL, Knotts TA, Chavez JA, Wang LP, Hoehn KL, Summers SA. Lipid mediators of insulin resistance. Nutr Rev 2007;65:S39–S46. [PubMed: 17605313]
78. Kraegen EW, Cooney GJ. Free fatty acids and skeletal muscle insulin resistance. Curr Opin Lipidol 2008;19:235–241. [PubMed: 18460913]

79. Wang G, Silva J, Dasgupta S, Bieberich E. Long-chain ceramide is elevated in presenilin 1 (PS1M146V) mouse brain and induces apoptosis in PS1 astrocytes. Glia 2008;56:449–456. [PubMed: 18205190]
80. Arboleda G, Huang TJ, Waters C, Verkhratsky A, Fernyhough P, Gibson RM. Insulin-like growth factor-1-dependent maintenance of neuronal metabolism through the phosphatidylinositol 3-kinase-Akt pathway is inhibited by C2-ceramide in CAD cells. Eur J Neurosci 2007;25:3030–3038. [PubMed: 17561816]
81. Gallou-Kabani C, Vige A, Gross MS, Rabes JP, Boileau C, Larue-Achagiotis C, Tome D, Jais JP, Junien C. C57BL/6J and A/J mice fed a high-fat diet delineate components of metabolic syndrome. Obesity (Silver Spring) 2007;15:1996–2005. [PubMed: 17712117]
82. Ito M, Suzuki J, Sasaki M, Watanabe K, Tsujioka S, Takahashi Y, Gomori A, Hirose H, Ishihara A, Iwaasa H, Kanatani A. Development of nonalcoholic steatohepatitis model through combination of high-fat diet and tetracycline with morbid obesity in mice. Hepatol Res 2006;34:92–98. [PubMed: 16423558]
83. Strissel KJ, Stancheva Z, Miyoshi H, Perfield JW 2nd, DeFuria J, Jick Z, Greenberg AS, Obin MS. Adipocyte death, adipose tissue remodeling, and obesity complications. Diabetes 2007;56:2910–2918. [PubMed: 17848624]
84. Diehl AM. Lessons from animal models of NASH. Hepatol Res 2005;33:138–144. [PubMed: 16198624]
85. Solis, Herruzo JA.; Garcia, Ruiz I.; Perez, Carreras M.; Munoz, Yague MT. Non-alcoholic fatty liver disease. From insulin resistance to mitochondrial dysfunction. Rev Esp Enferm Dig 2006;98:844–874. [PubMed: 17198477]
86. Soscia SJ, Tong M, Xu XJ, Cohen AC, Chu J, Wands JR, de la Monte SM. Chronic gestational exposure to ethanol causes insulin and IGF resistance and impairs acetylcholine homeostasis in the brain. Cell Mol Life Sci 2006;63:2039–2056. [PubMed: 16909201]
87. Lopes-Cardozo M, Sykes JE, Van der Pal RH, van Golde LM. Development of oligodendrocytes. Studies of rat glial cells cultured in chemically-defined medium. J Dev Physiol 1989;12:117–127. [PubMed: 2696749]
88. Broughton SK, Chen H, Riddle A, Kuhn SE, Nagalla S, Roberts CT Jr, Back SA. Large-scale generation of highly enriched neural stem-cell-derived oligodendroglial cultures: maturation-dependent differences in insulin-like growth factor-mediated signal transduction. J Neurochem 2007;100:628–638. [PubMed: 17263792]
89. Chesik D, De Keyser J, Wilczak N. Insulin-like growth factor system regulates oligodendroglial cell behavior: therapeutic potential in CNS. J Mol Neurosci 2008;35:81–90. [PubMed: 18299999]

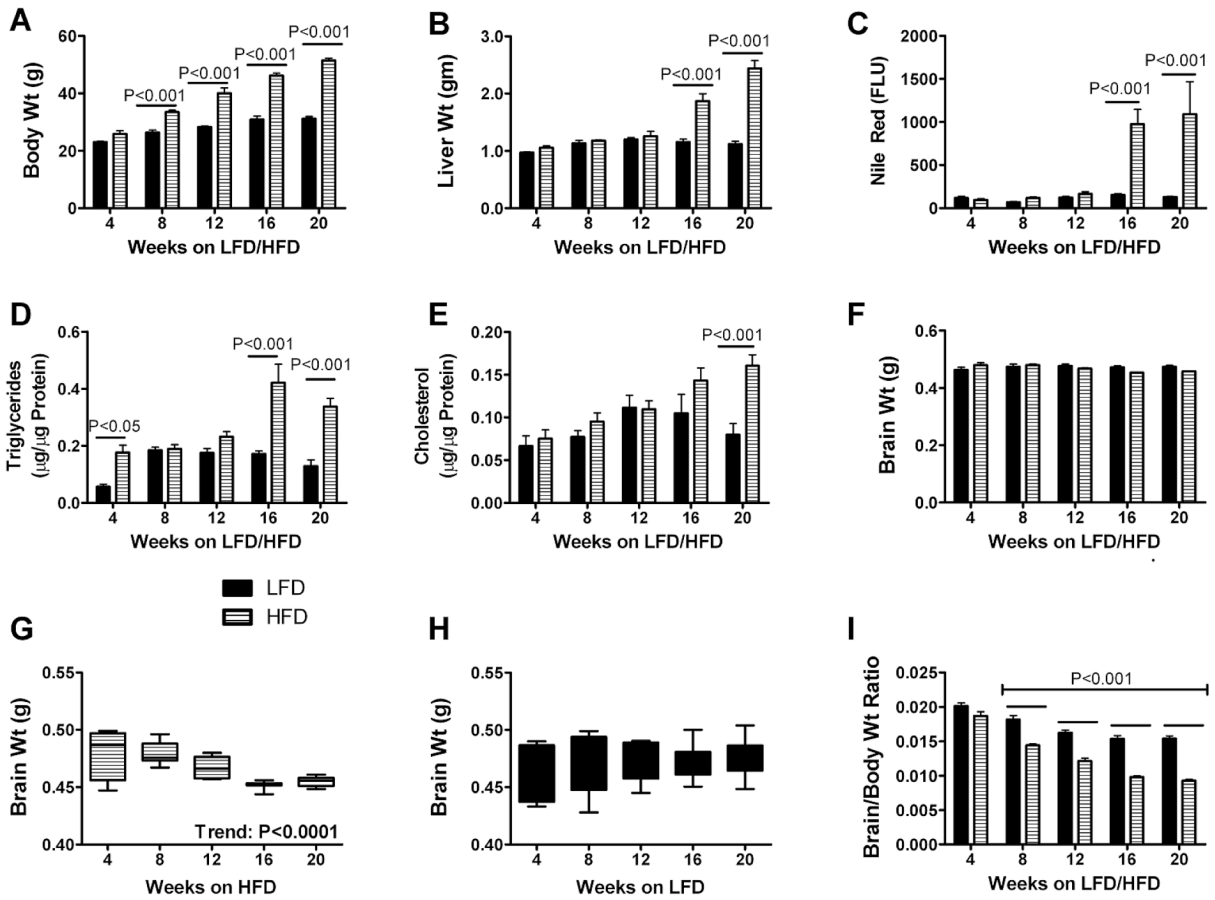

Fig. 1.

Effects of high fat diet (HFD) feeding on body, liver, and brain weight, and hepatic lipid content. Adult male C57BL/6 mice were fed with high fat (HFD) or low fat (LFD) chow diets for 4, 8, 12, 16, or 20 weeks (N = 10/group). Bar graphs or box plots depict mean ± range and/or S.E.M. for (A) body weight, (B) liver weight, (C) Nile Red fluorescence measurement of liver lipid content, (D) hepatic triglyceride levels, (E) hepatic cholesterol levels, (F) brain weight, (G, H) brain weight trend over time for mice fed with the (G) HFD or (H) LFD, and (I) the calculated brain/body weight ratio for each group at the time of sacrifice. Inter-group comparisons were made using Two-way ANOVA with the post-hoc Bonferroni test of significance, or within-group trend analysis. Significant P-values and trends are indicated within the panels.

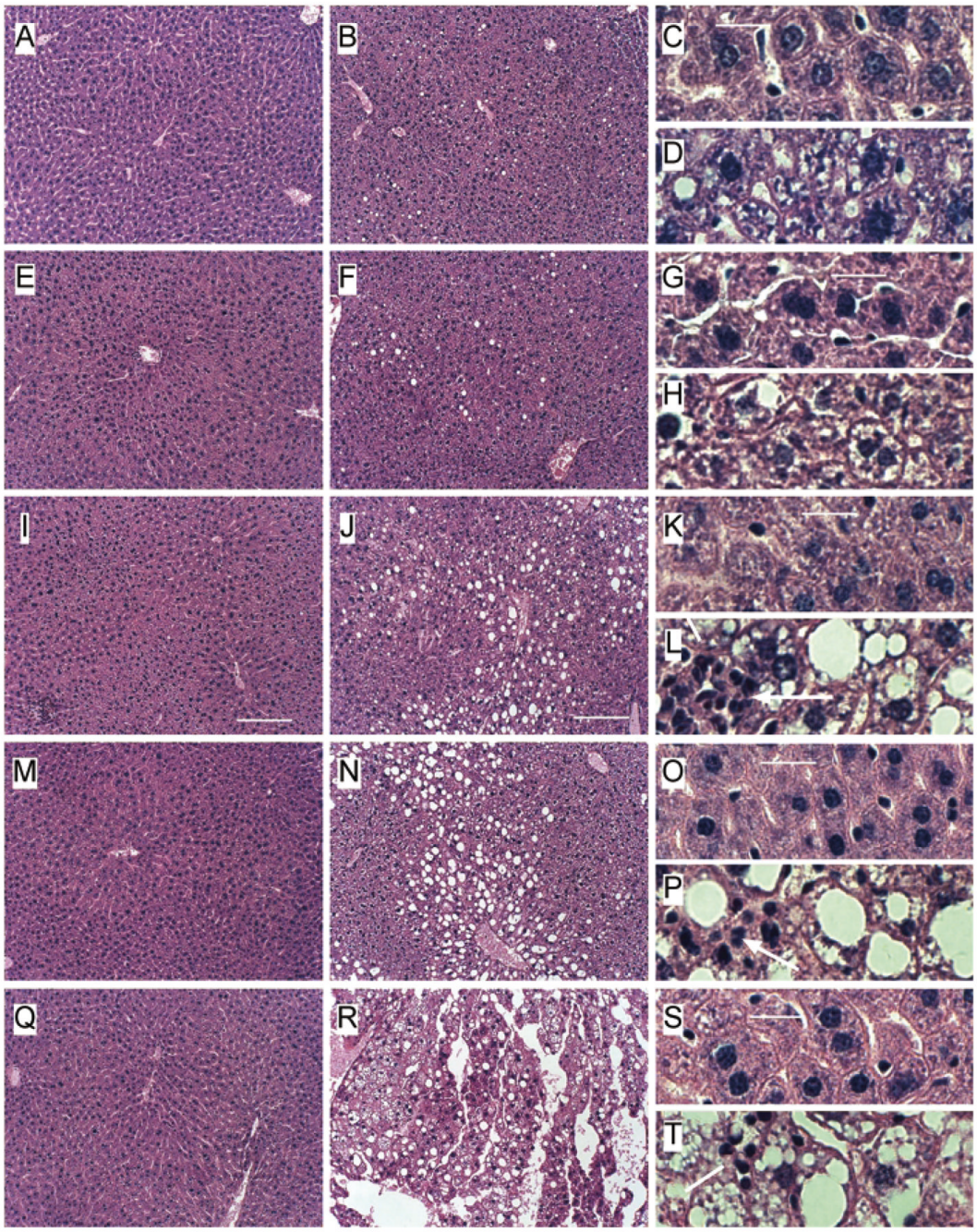

Fig. 2.

Chronic HFD feeding causes NASH. Adult male C57BL/6 mice were fed with high fat (HFD) or low fat (LFD) chow for 4, 8, 12, 16, or 20 weeks (N = 10/group). Liver tissue harvested at sacrifice was fixed in Histochoice, embedded in paraffin, and histological sections were stained with H&E. Photomicrographs depict representative areas of liver from mice maintained for 4 (A–D), 8 (E–H), 12 (I–L), 16 (M–P) or 20 (Q–T) weeks on the LFD (A,C,E,G,I,K,M,O,Q,S) or HFD (B,D,F,H,J,L,N,P,R,T). Over time, mice fed with the LFD exhibited no detectable change in liver histology, whereas mice fed with the HFD exhibited progressive increases in steatosis (marked by clear intracellular vacuoles) that was detectable after just 4 weeks of HFD feeding (D), and associated with inflammation (arrows) and cell loss (reduced hepatocyte

nuclear density) beginning at the 12 week time point. Note extensive macro- and microsteatosis with reduced hepatocellular nuclei in Panels P and T relative to O and S. Original magnifications, A,B,E,F,I,J,M,N,Q,R = 200x; C,D,G,H,K,L,O,P,S,T= 1200x. Scale bar = 50 μm. (Colours are visible in the electronic version of the article at www.iospress.nl.)

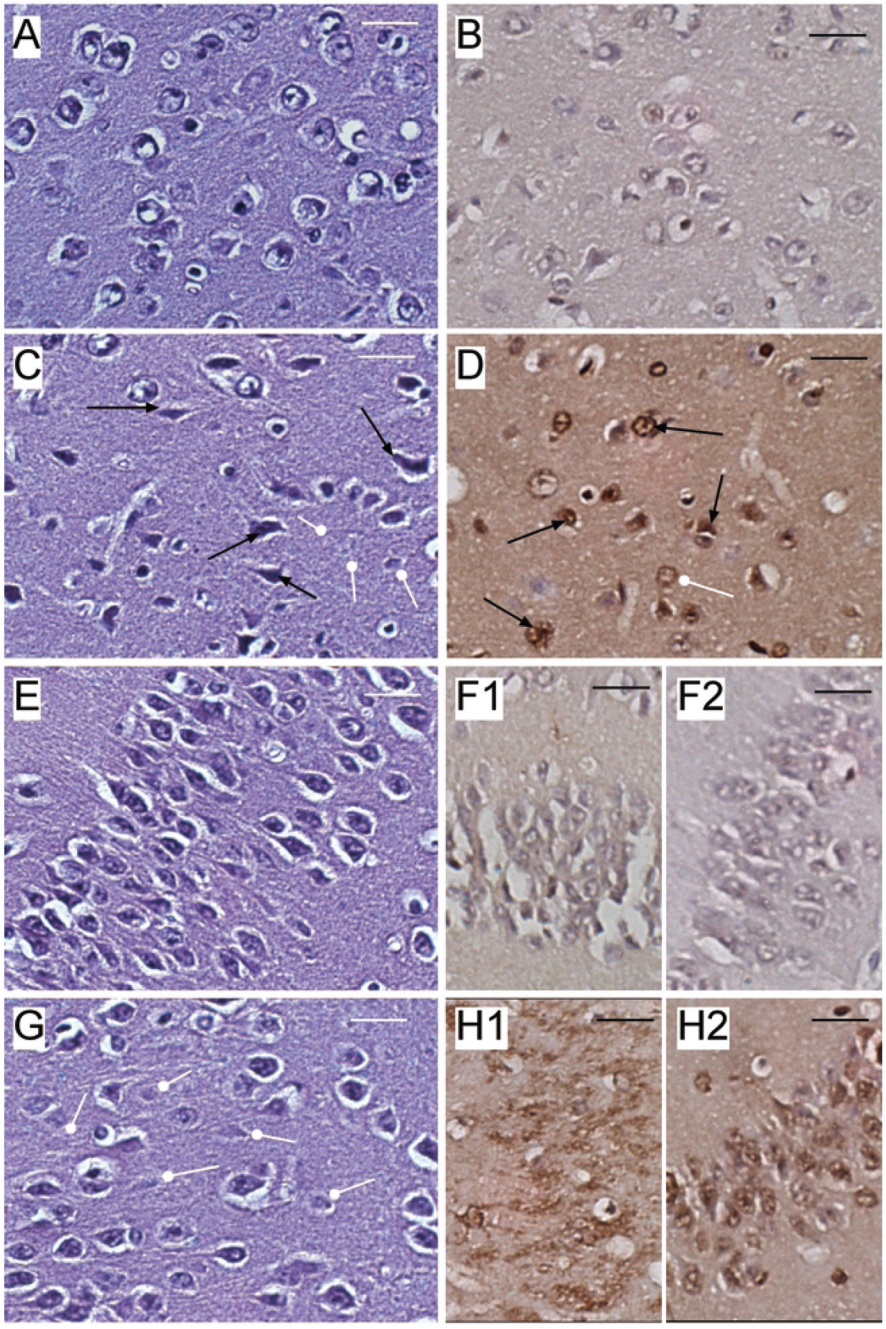

Fig. 3.

Neurodegeneration in diet Induced obesity with T2DM and NASH. Adult male C57BL/6 mice were fed with low fat (LFD-A,B,E,F1,F2) or high fat (HFD-C,D,G,H1,H2) chow for 20 weeks (N = 10/group). Brains harvested at sacrifice was immersion fixed in Histochoice, embedded in paraffin, and adjacent histological sections including (A–D) temporal cortex and (E–H) hippocampal formation (CA1), were either stained with (A,C,E,G) Luxol Fast Blue, H&E,or immunostained with antibodies to (B,D,F2,H2) 4-hydroxynonenal (4-HNE) or (F1,H1) glial fibrillary acidic protein (GFAP) to detect lipid peroxidation/oxidative stress or gliosis, respectively. Immunoreactivity was detected by the ABC method with diaminobenzidine as the chromagen. Immunostained sections were lightly counterstained with Hematoxlin. HFD

fed mice exhibited reduced cell density with ongoing neuronal shrinkage (black arrows) and apoptosis (white wands) in the (C) temporal cortex and (G) hippocampal formation, relative to corresponding brain regions in (A,E) LFD fed mice. Ongoing cell loss was associated with increased 4-HNE (arrows) and GFAP immunoreactivity in the temporal cortex and/or hippocampal formation in (D,H) HFD relative to (B,F) LFD fed mice. Original magnifications, 600x for all images. Scale bar = 50 μm. (Colours are visible in the electronic version of the article at www.iospress.nl.)

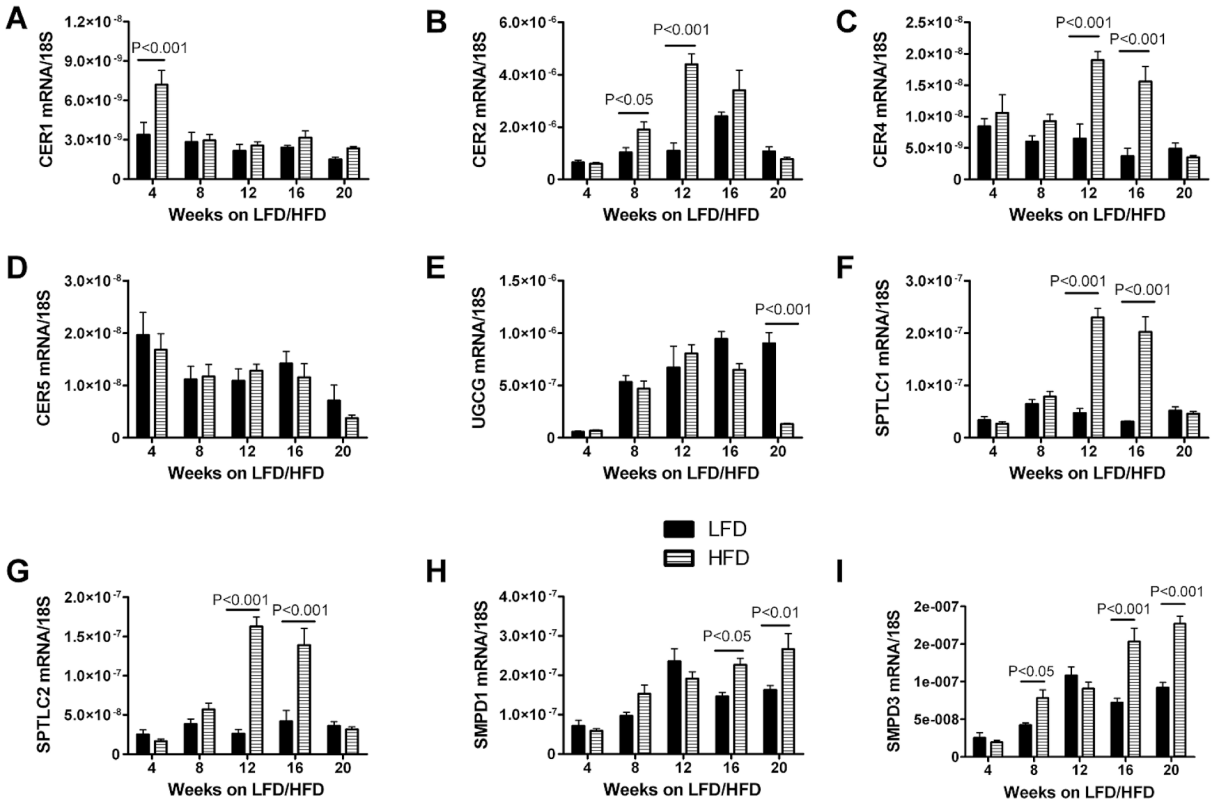

Fig. 4.

Effect of HFD feeding on pro-ceramide gene expression in liver. Total RNA extracted from liver was reverse transcribed using random oligodeoxynucleotide primers, and the resulting cDNA templates were used in qRT-PCR assays to measure (A) Ceramide synthase (CER)1, (B) CER2, (C) CER4, (D) CER5, (E) UDP-glucose ceramide glycoysltransferase (UGCG), (F) Serine palmitoyltransferase 1 (SPTLC1), (G) SPTLC2, (H) sphingomyelin phosphodiesterase 1 (SMPD1), and (I) SMPD3. The mRNA levels were normalized to 18S rRNA measured in the same templates. Graphs depict the mean ± S.E.M. levels of gene expression in brains from LFD-fed or HFD-fed mice (N = 6/group; see Material and Methods). Inter-group comparisons were made using Two-way ANOVA with the post-hoc Bonferroni test of significance. Significant P-values are indicated within the panels.

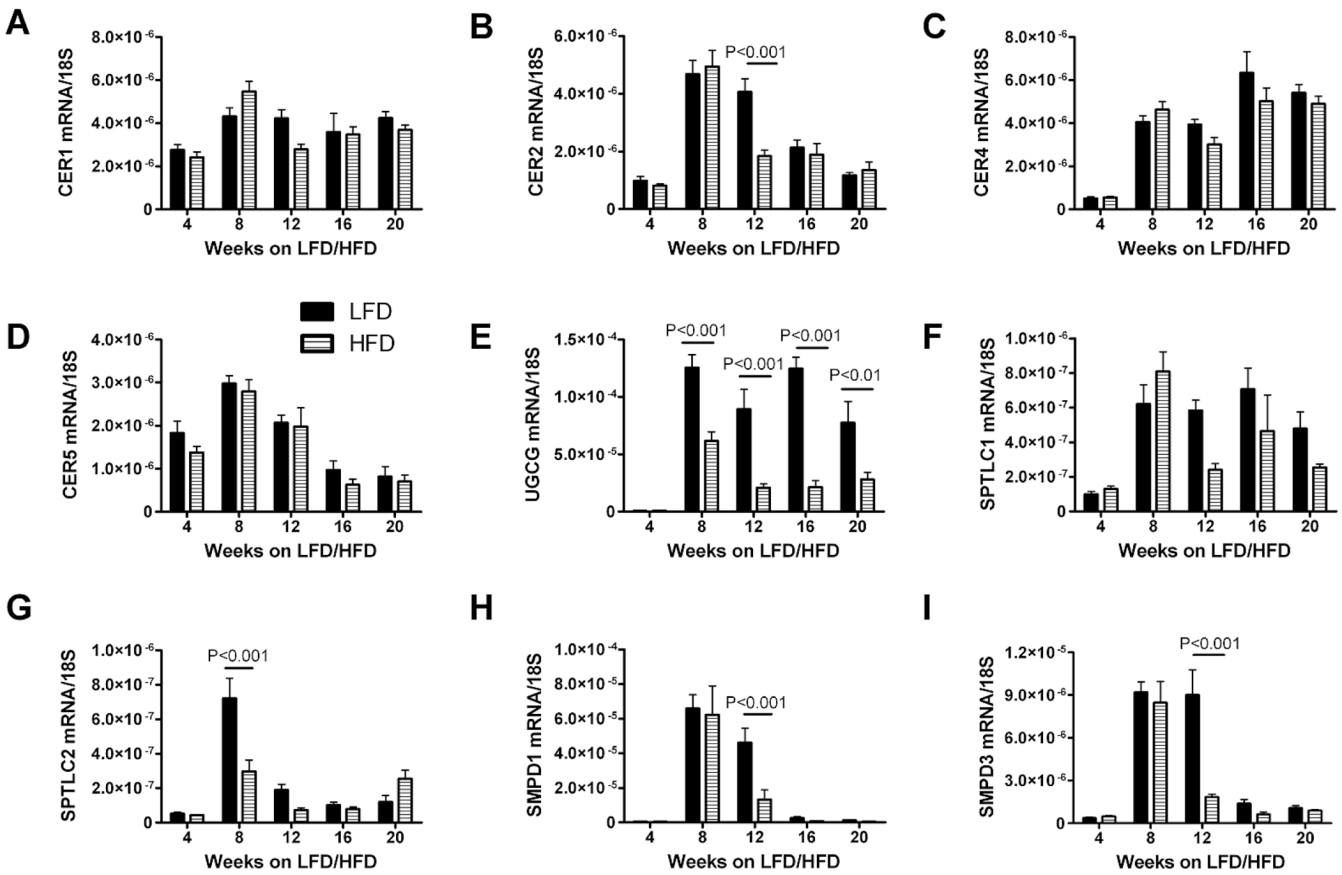

Fig. 5.

Effect of HFD feeding on pro-ceramide gene expression in temporal lobe. Total RNA extracted from liver was reverse transcribed using random oligodeoxynucleotide primers, and the resulting cDNA templates were used in qRT-PCR assays to measure (A) Ceramide synthase (CER)1, (B) CER2, (C) CER4, (D) CER5, (E) UDP-glucose ceramide glycoysltransferase (UGCG), (F) Serine palmitoyltransferase 1 (SPTLC1), (G) SPTLC2, (H) sphingomyelin phosphodiesterase 1 (SMPD1), and (I) SMPD3. The mRNA levels were normalized to 18S rRNA measured in the same templates. Graphs depict the mean ± S.E.M. levels of gene expression in brains from LFD-fed or HFD-fed mice (N = 6 per group; see Material and Methods). Inter-group comparisons were made using Two-way ANOVA with the post-hoc Bonferroni test of significance. Significant P-values are indicated within the panels.

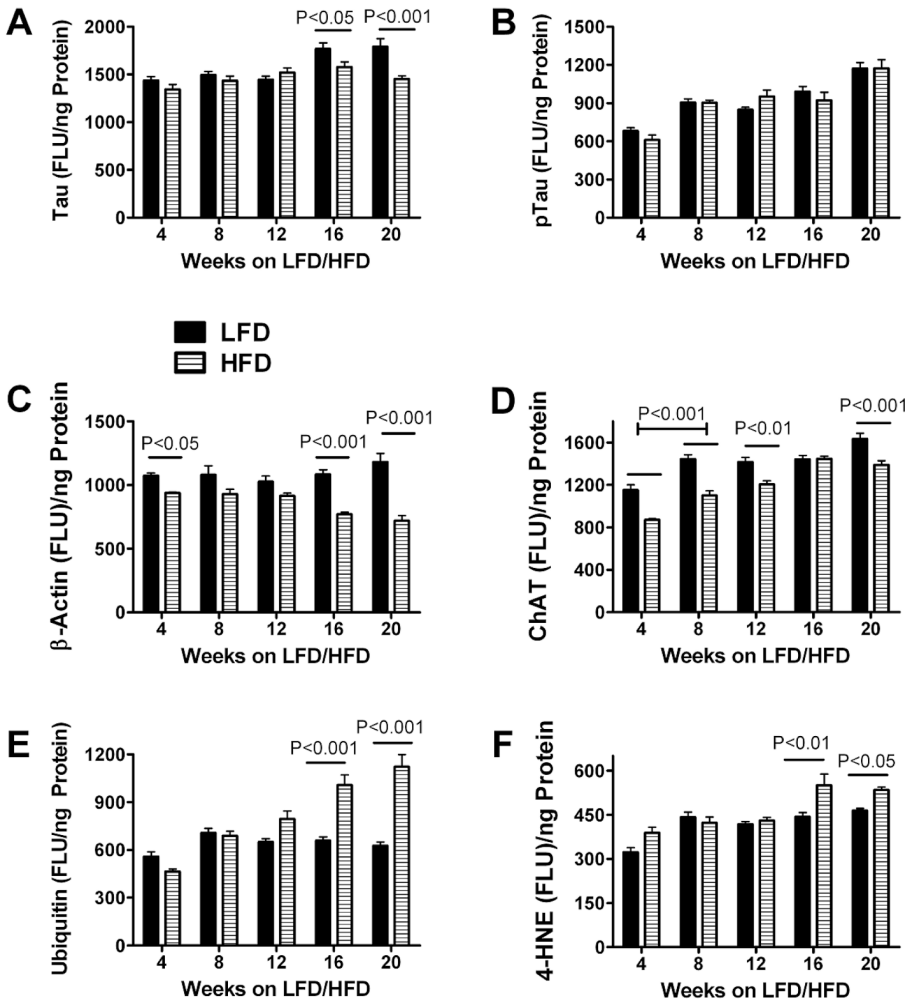

Fig. 6.

Effect of HFD feeding on molecular indices of neurodegeneration. Temporal lobe protein homogenates from LFD-fed or HFD-fed mice were used to measure (A) tau; (B) phospho (p)-tau; (C) β-actin; (D) choline acetyltransferase (ChAT); (E) ubiquitin; and (F) 4-hydroxynonenal (4-HNE) by ELISA (see Materials and Methods). Immunoreactivity was detected with HRP-conjugated secondary antibody and Amplex Red soluble fluorophor. Fluorescence light units (FLU) were measured (Ex 579 nm/Em 595 nm) in a Spectromax M5, and results were normalized to sample protein content in the wells. Graphs depict mean ± S.E.M of results (N = 8/group). Inter-group comparisons were made using Two-way ANOVA with the post-hoc Bonferroni test of significance. Significant P-values are indicated within the panels.

Table 1

Ceramide related genes and their functions

Gene	Abbreviation/Synonym	Molecular pathway	Effect/References
Serine palmitoyltransferase	SPTLC: 1. SPTLC-1: subunit 1 (non catalytic) 2. SPTLC-2: Subunit 2 (catalytic)	Rate limiting step in *de novo* ceramide synthesis from condensation of serine and palmitoyl-CoA	References: #44, #45, #54
Sphingomyelin phosphodiesterase 1, acid lysosomal	SMPD1, aSMase, A-SMase	Ceramide generation from acid sphingomyelinase –dependent hydrolysis of sphingomyelin	References: #44, #52
Sphingomyelin phosphodiesterase 3, neutral	SMPD3, nSMase2	Ceramide generation from neutral sphingomyelinase –dependent hydrolysis of sphingomyelin	References: #44, #51
Ceramide synthase 1	LAG1 homolog, ceramide synthase 1 (Lass1)	*De novo* synthesis from N-acylation of spingosine	Synthesis of C18-ceramide #47
Ceramide synthase 2	LAG1 homolog, ceramide synthase 2 (Lass2)	*De novo* synthesis from N-acylation of spingosine	Synthesis of C20-C26 ceramide. Reference: #47
Ceramide synthase 4	LAG1 homolog, ceramide synthase 4 (Lass4)	*De novo* synthesis from N-acylation of spingosine	Synthesis of C18, C20, C24 References: #47, #53
Ceramide synthase 5	LAG1 homolog, ceramide synthase 5 (Lass5), CerS5	*De novo* synthesis from N-acylation of spingosine	Synthesis of C16-ceramide References: #47, #44
UDP-glucose ceramide glucosyltransferase	UGCG	First step in glycosphingolipid synthesis, the transfer of glucose from UDP-glucose to ceramide.	Synthesis of glucosylceramide References: #56, #57

J Alzheimers Dis. Author manuscript; available in PMC 2010 June 28.

Table 2

List of primer pairs used for qPCR studies

Gene-Specific Primer	Forward/ Reverse	Sequence 5'-3'	Position (mRNA)	Amplicon	TM
18S rRNA	Forward	GGACACGGACAGGATTGACA	1278	50	74.5
18S rRNA	Reverse	ACCCACGGAATCGAGAAAGA	1327		
SPTLC-1	Forward	TCGAGTTAAGGCCACAGCTT	357	74	76.3
SPTLC- 1	Reverse	CATAGAACCCTCGAGGACCA	430		
SPTLC-2	Forward	GGATACATCGGAGGCAAGAA	1209	80	79.3
SPTLC-2	Reverse	GACATCGACGTGGCATACAC	1288		
CERS1	Forward	CGTAAGGACTCGGTGGTCAT	547	68	80.9
CERS1	Reverse	GCGTAGGAAGAGGCAATGAG	614		
CERS2	Forward	GTTTAACTACGCGGGATGGA	855	55	75.4
CERS2	Reverse	GGCGAACACAATGAAGAGGT	909		
CERS4	Forward	GATGAAGCCTCTCTGCTGCT	1889	60	79.0
CERS4	Reverse	AGGACACCCACAGGTTTCTG	1948		
CERS5	Forward	CATGCCATCTGGTCCTACCT	1106	85	80.7
CERS5	Reverse	CATCACTGCGGTCATCCTTA	1190		
UGCG	Forward	TGGGACCCGACTATAAGCTG	1199	73	80.1
UGCG	Reverse	CCAGGATCTCCTCTGCTGTC	1271		
SMPD-1	Forward	CAGTTCTTTGGCCACACTCA	1469	65	75.6
SMPD-1	Reverse	CGGCTCAGAGTTTCCTCATC	1533		
SMPD-3	Forward	CTGACTCCAGACAGCATCCA	3604	72	80.0
SMPD-3	Reverse	ACTGTGCTGAGCTTGGGACT	3675		

List of abbreviations: qPCR = quantitative polymerase chain reaction; SPTLC = serine palmitoyl transferase; CerS = ceramide synthase; SMPD = sphingomyelinase; UGCG = UDP-glucose ceramide glucosyltransferae.